Modelling framework for asynchronous land-atmosphere coupling using NASA GISS ModelE and LPJ-LMfire: Design, Application and Evaluation for the 2.5ka period

Ram Singh[1,2], Alexander Koch[4], Allegra N LeGrande[2,1], Kostas Tsigaridis[1,2], Riovie D Ramos[5], Francis Ludlow[6], Igor Aleinov[1,2], Reto Ruedy[2,3], Jed O. Kaplan[7]

[1] Center for Climate Systems Research, Columbia University, New York, USA

[2] NASA Goddard Institute for Space Studies, New York, NY-10025, USA

[3] SciSpace LLC, New York, NY, USA

[4] Department of Earth Sciences, The University of Hong Kong, Hong Kong SAR, China

[5] Earth Observatory of Singapore, Singapore

[6] Department of History, School of Histories and Humanities, Trinity College, Dublin 2, Ireland

[7] Department of Earth, Energy, and Environment, University of Calgary, Calgary AB, Canada

Correspondence to: Ram Singh (ram.bhari85@gmail.com)

Supplementary Results and Information

GISS Ent PFTs

1.) Evergreen Broadleaf Early Succ

2.) Evergreen Broadleaf Late Succ

3.) Evergreen Needleleaf Early Succ

4.) Evergreen Needleleaf Late Succ

5.) Cold Deciduous Broadleaf Early Succ

6.) Cold Deciduous Broadleaf Late Succ

7.) Drought Deciduous Broadleaf

8.) Deciduous Needleleaf

9.) Cold Adapted Shrub

10.) Arid Adapted Shrub

11.) C3 Grass Perennial

12.) C4 Grass

13.) C3 Grass Annual

14.) Arctic C3 Grass

15.) Crops Herb

16.) Crops Woody

17.) Bright Bare Soil

18.) Dark Bare Soil

LPJ PFTs

1.) tropical broadleaf evergreen

2.) tropical broadleaf raingreen

3.) temperate needleleaf evergreen

4.) temperate broadleaf evergreen

5.) temperate broadleaf summergreen

6.) boreal needleleaf evergreen

7.) boreal summergreen

8.) C3 perennial grass

9.) C4 perennial grass

Ent PFTs	LtoG_M0	LtoG_M1 **(M1)**	LtoG_M2 **(M2)**
1	Not Used	Not Used	Not Used
2	1 + 4	1 + 4	1 + 4
3	Not used	Not used	Not used
4	3 + 6	3 + 6	3 + 6
5	Not used	Not used	Not used
6	5(>10 m) +7 (>15 m){6 present}	5 (>12 meters) + 7 (>12m)	5 (>11m) + 7 (>11m) {6 present}
7	2 for height > 10m	2 for height > 15m	2 for height > 11m
8	7 for height > 15m {6 absent}	7 for height > 12m	7 for height > 11m {6 absent}
9	7 for height ≤ 15m+ (0.4x8) (where PFT 7 is absent)	7 for height ≤ 12m + (0.5x8) (where PFT 7 is absent)	7 for height ≤ 11m
10	2+5 for height ≤ 10m + (0.4x8) (where PFT 7* is absent)	2+5 for height ≤ 12m + (0.5x8) (where PFT 7* is absent)	2+5 for height ≤ 11m
11	0.3 x 8	0.25 x 8	0.5 x 8
12	9	9	9
13	0.3 x 8	0.25 x 8	0.5 x 8
14	conditional 8 (only where PFT-8 is present, no other PFT)	conditional 8 (only where PFT-8 is present, no other PFT)	conditional 8 (only where PFT-8 is present, no other PFT)
15	NO	NO	NO
16	NO	NO	NO
17*	(1-Vtotal)x0.7	(1-Vtotal)x0.7	(1-Vtotal)x0.7
18*	(1-Vtotal)x0.3	(1-Vtotal)x0.3	(1-Vtotal)x0.3

*Soils are redistributed based on ratio of bright & dark soil in GISS present-day vegetation.
*Vtotal stands for total vegetation cover over a grid cell.
*PFT-7 is assigned to cold shrub.

Table S1: The three mapping schemes defines the Vegetation cover distribution for each PFT type among 3 mapping schemes and comparison with GISS Ent distribution. Numeric in the table refers to the PFT type listed above. “LtoG_M” stands for LPJ to GISS mapping and integer following denote the number of mapping scheme.

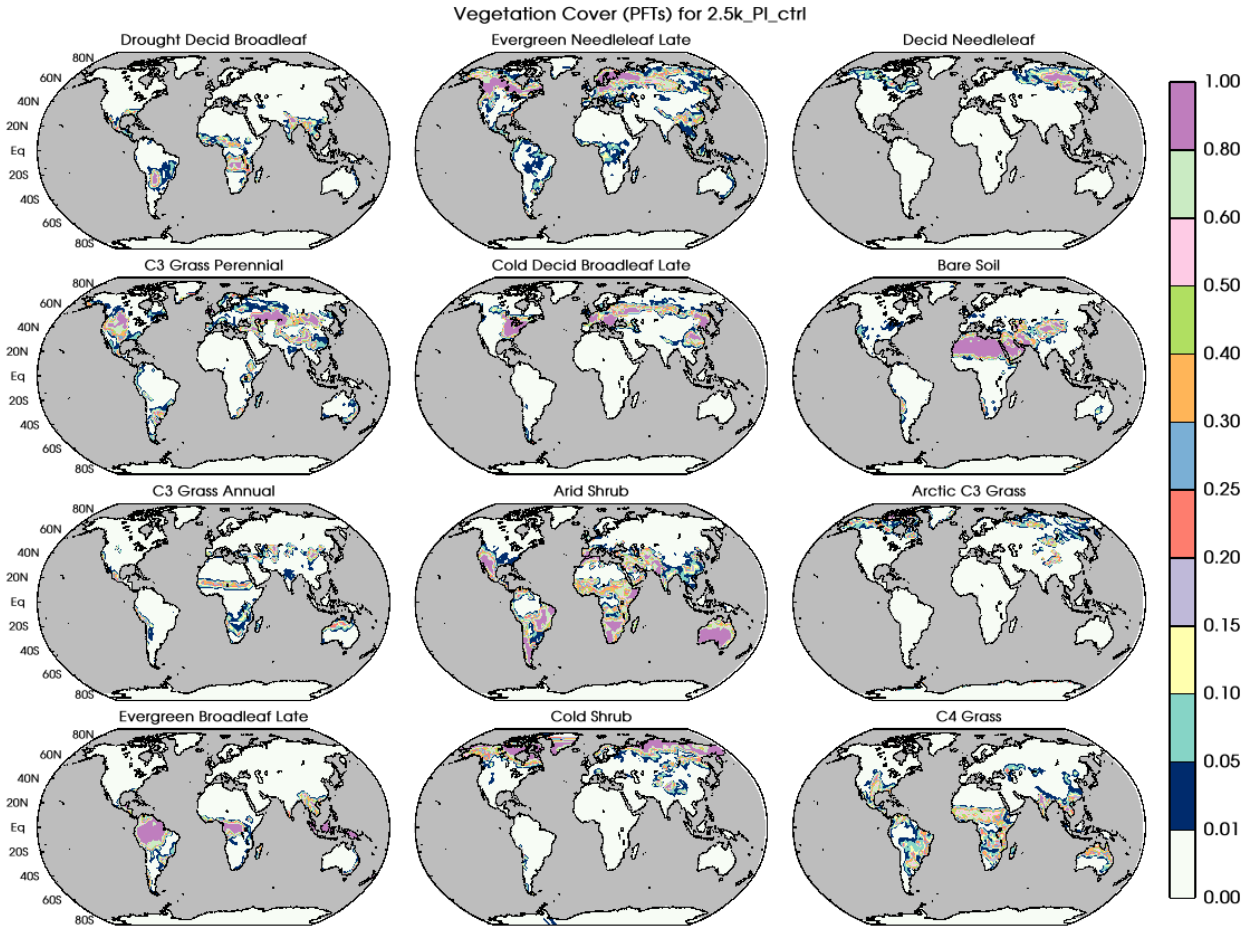

Figure S1.A: Vegetation cover used for the ModelE preindustrial control run. Dark and bright bare soils are shown combined as total bare soil.

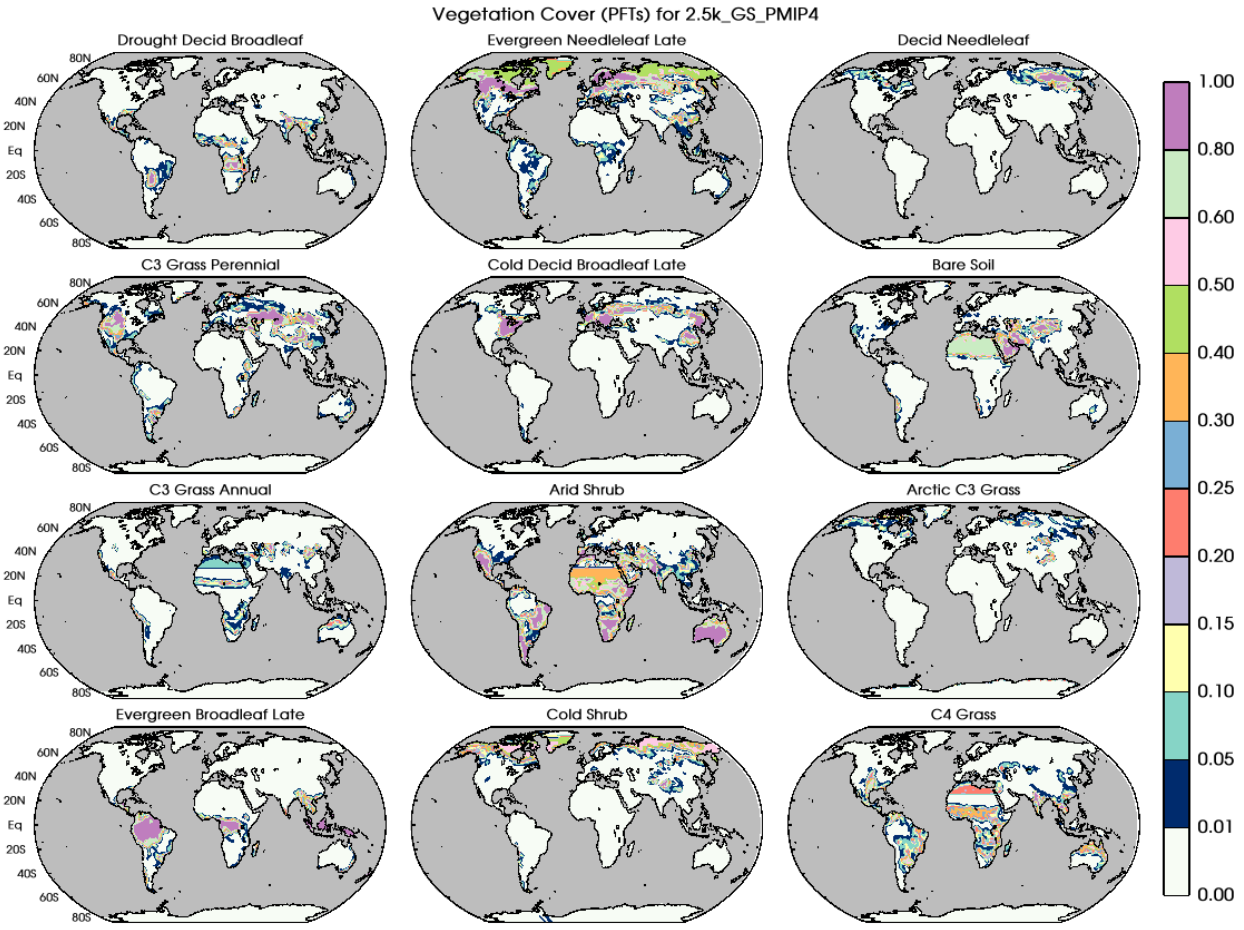

Figure S1.B: Vegetation cover used for the ModelE 2.5ka control run. This includes a linearly-interpolated vegetation cover specified from the mid-Holocene green Sahara conditions as designed under PMIP4 protocols (Otto-Bliesner et al., 2017). Dark and bright bare soils are shown combined as total bare soil.

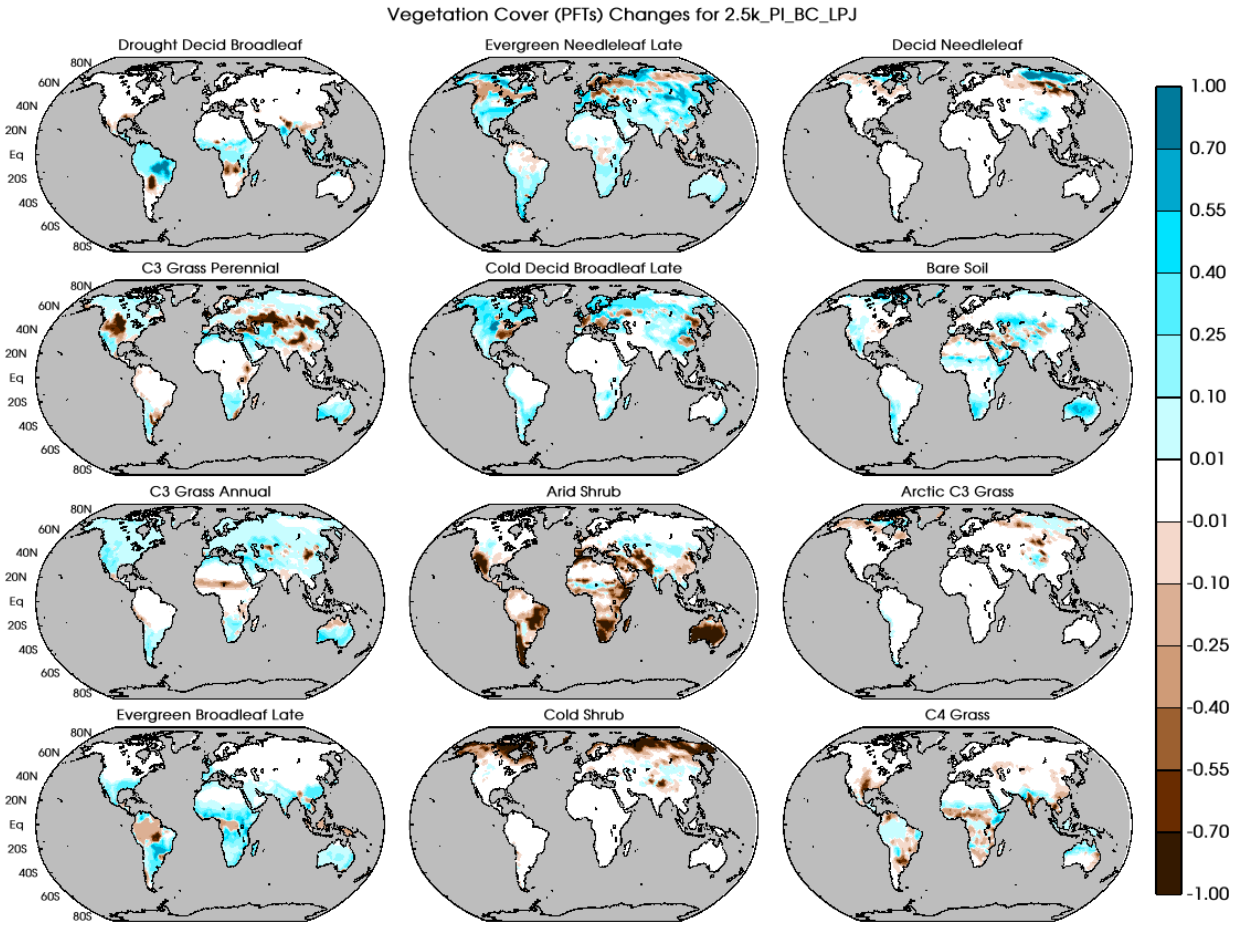

Fig S2.A. Changes in the various PFTs using the LPJ-LMfire simulated vegetation distribution for the 2.5ka period under the LtoG_M2 **(M2) (Table S1)** mapping scheme after the final iteration when a bias correction is applied, and with the interannual variability form LPJ-LMfire.

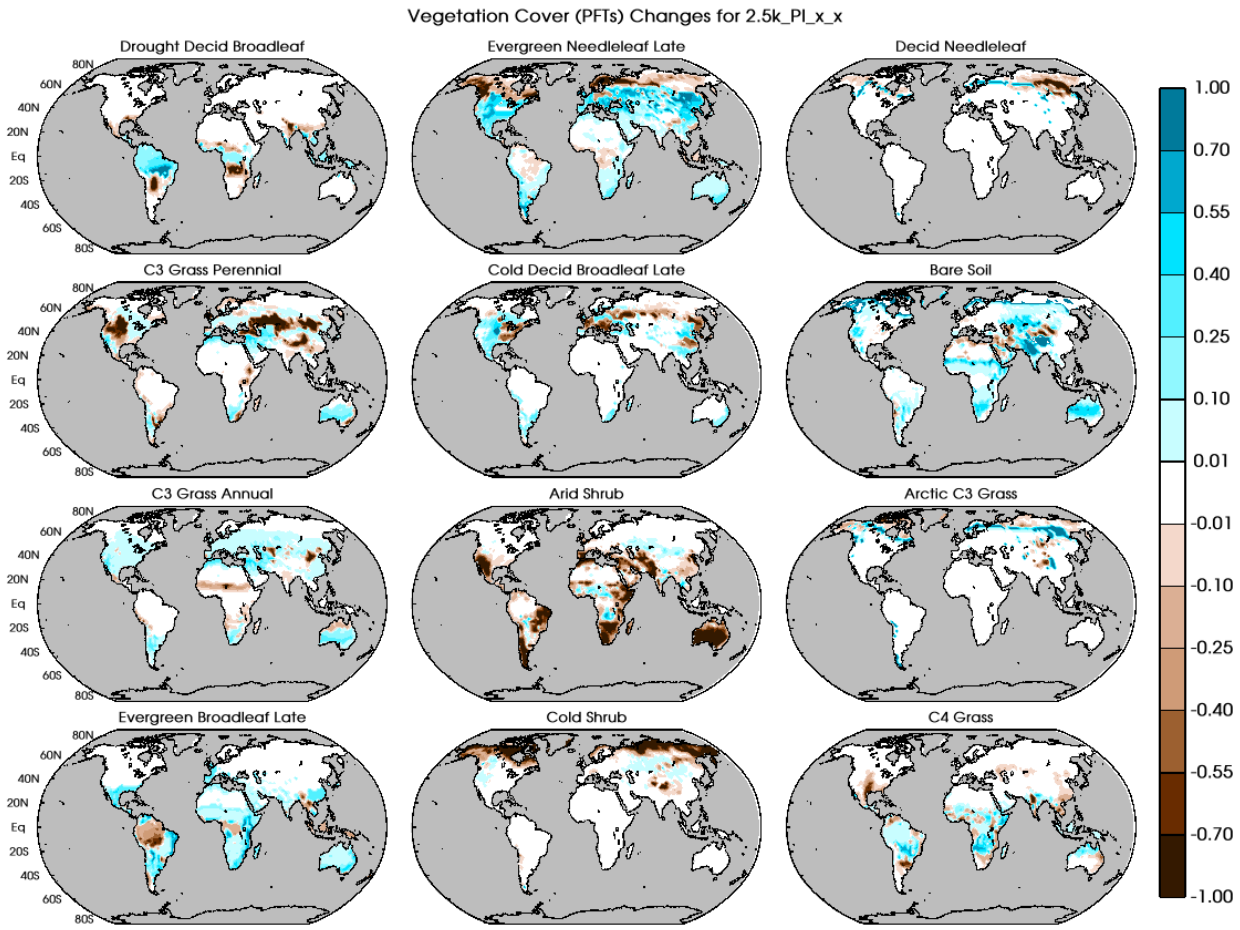

Fig S2.B. Same as Figure S2.A without using a bias correction and an interannual variability.

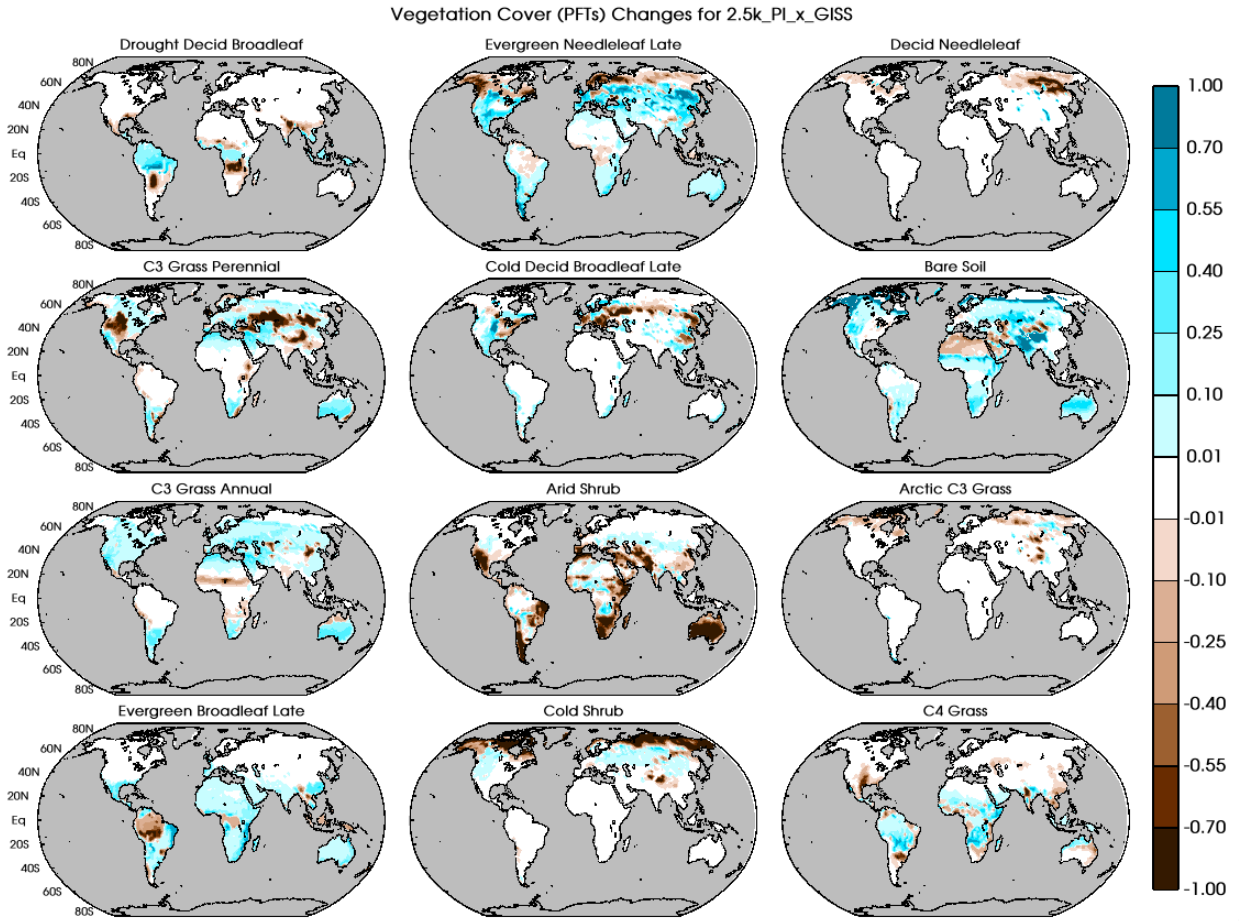

Fig S2.C. Same as in Fig. S2.A, without bias correction and with the interannual variability from ModelE.

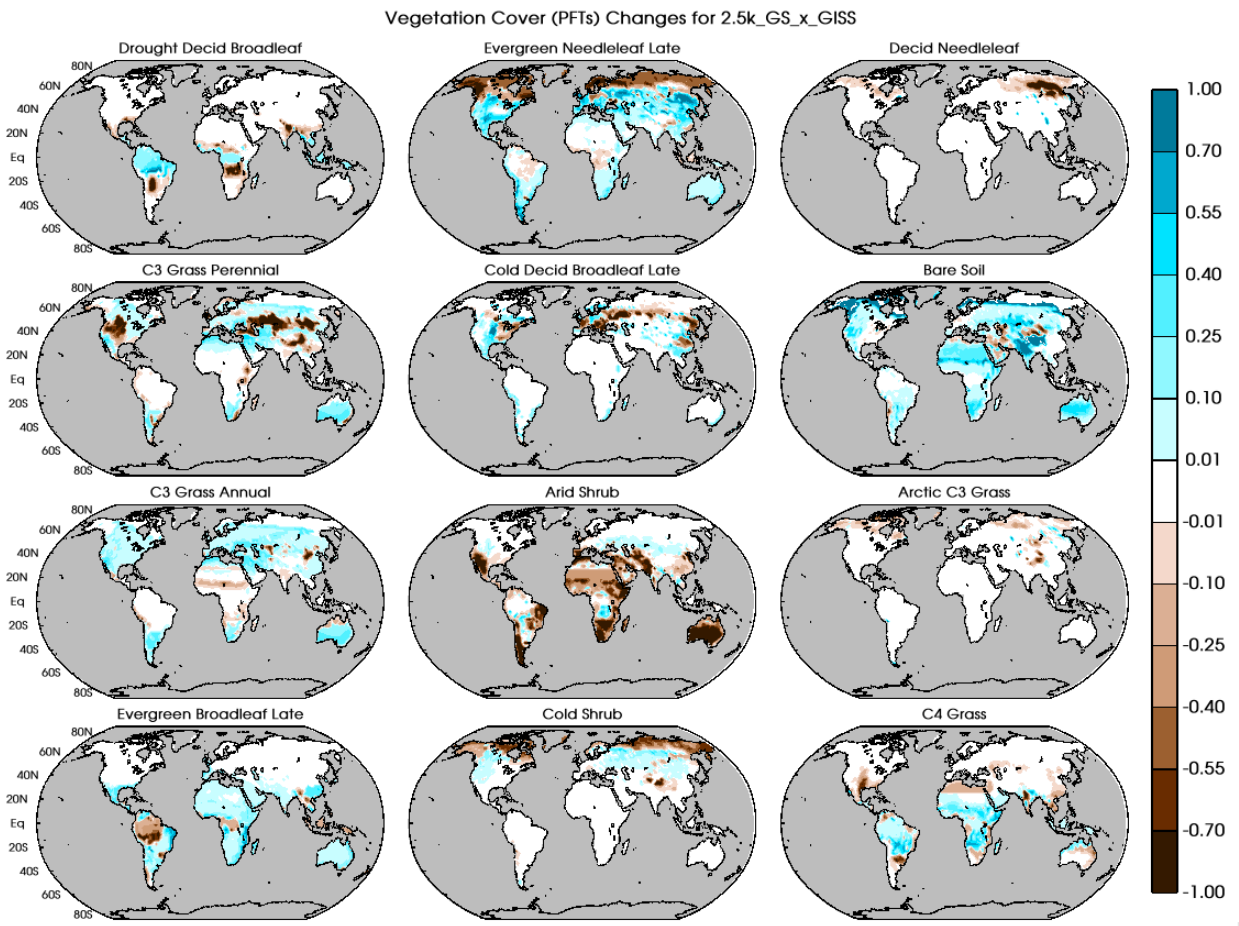

Fig S2.D. Same as in Fig. S2.C, using partially green Sahara conditions.

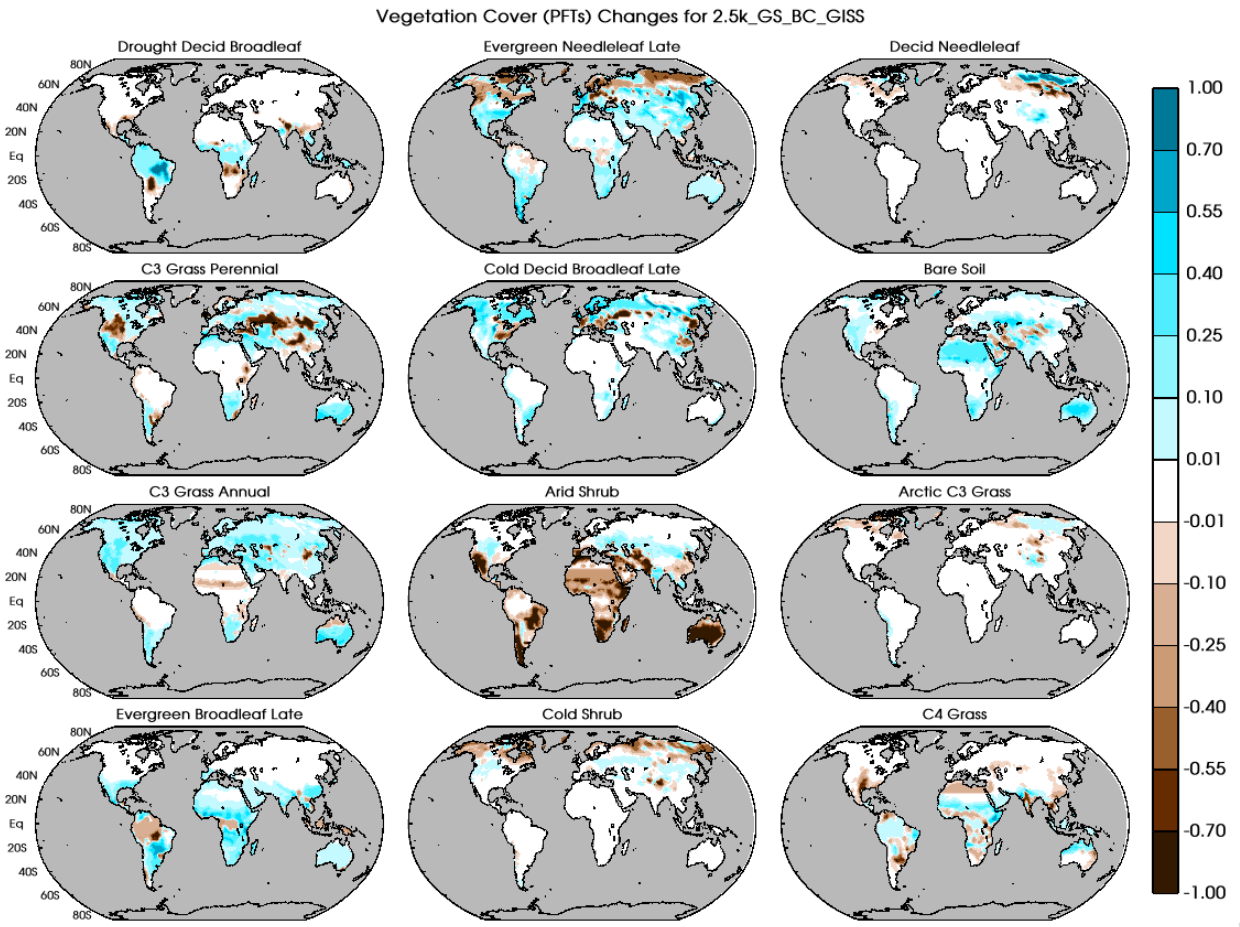

Fig S2.E: Same as in Fig. S2.D with bias correction.

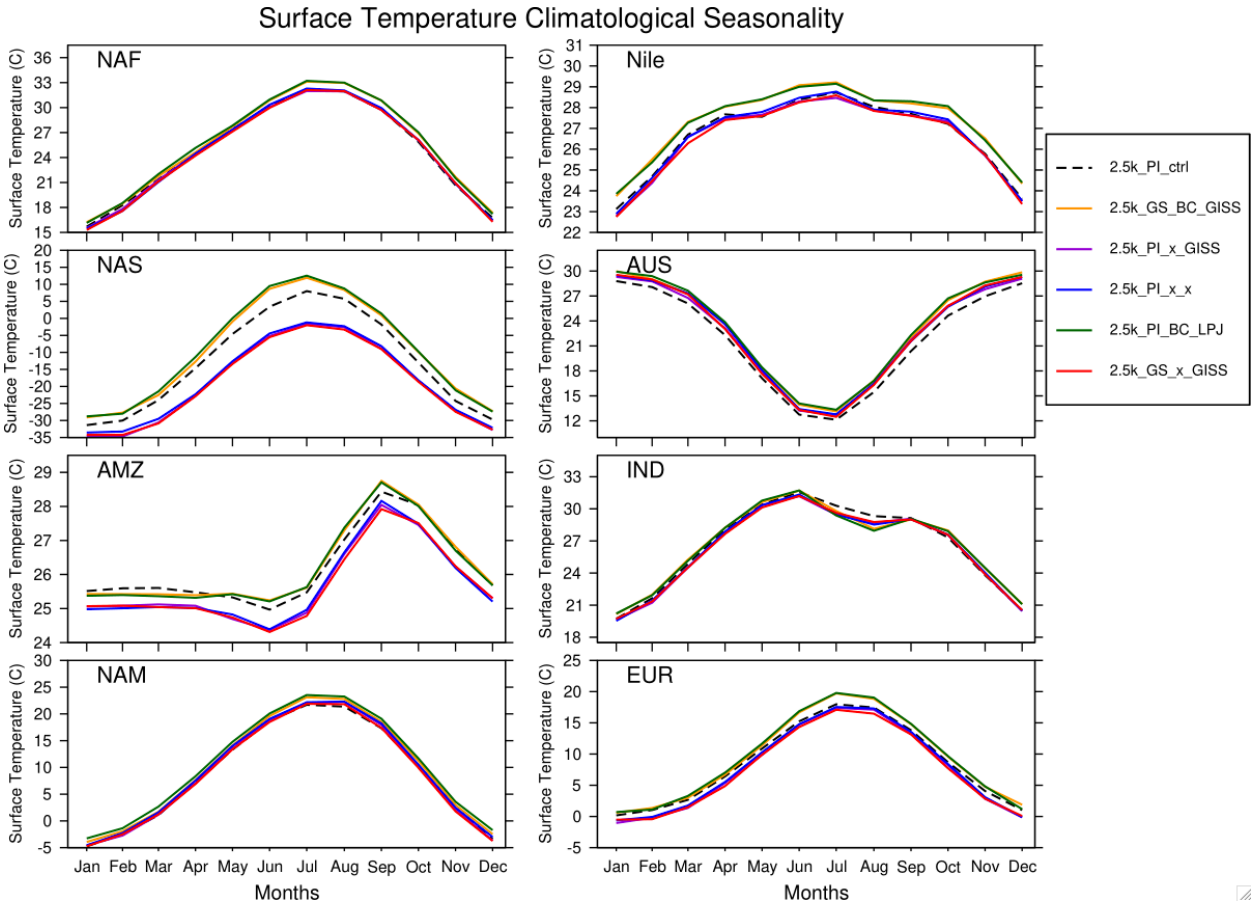

Figure S3: Seasonality of mean surface temperature over the selected regions.

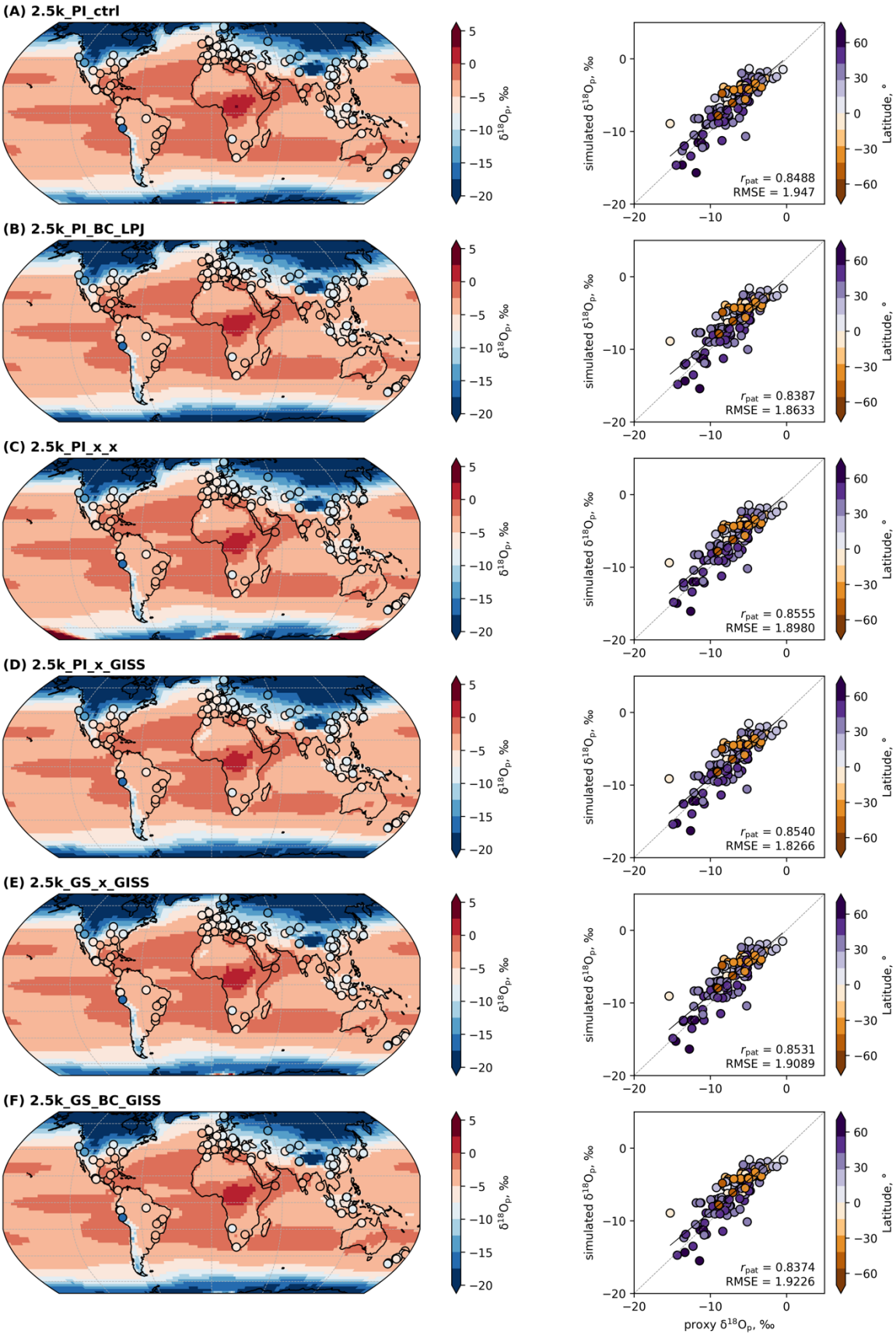
(A) 2.5k_PI_ctrl
(B) 2.5k_PI_BC_LPJ
(C) 2.5k_PI_x_x
(D) 2.5k_PI_x_GISS
(E) 2.5k_GS_x_GISS
(F) 2.5k_GS_BC_GISS
δ18Op, ‰
simulated δ18Op, ‰
proxy δ18Op, ‰
Latitude, °
rpat = 0.8488
RMSE = 1.947
rpat = 0.8387
RMSE = 1.8633
rpat = 0.8555
RMSE = 1.8980
rpat = 0.8540
RMSE = 1.8266
rpat = 0.8531
RMSE = 1.9089
rpat = 0.8374
RMSE = 1.9226

Figure S4. Comparison of simulated $\delta^{18}O_p$ with speleothem $\delta^{18}O$. Left column: global distribution (70° S-70° N) of simulated $\delta^{18}O_p$ (background) and speleothem $\delta^{18}O$ (circles), converted to their drip water equivalents (see text) for all simulations. Right column: scatterplots between simulated and proxy $\delta^{18}O_p$. Black lines represent the least squares regression fits to data points while the gray dashed lines represent the 1:1 line. r_{pat} and RMSE for each iteration are reported in the lower right corner of each scatterplot.